



Article

# Role of Salt Migration in Destabilization of Intra Permafrost Hydrates in the Arctic Shelf: Experimental Modeling

Evgeny Chuvilin <sup>1,\*</sup>, Valentina Ekimova <sup>1</sup>, Boris Bukhanov <sup>1</sup>, Sergey Grebenkin <sup>1</sup>, Natalia Shakhova <sup>2,3</sup> and Igor Semiletov <sup>2,3,4</sup>

<sup>1</sup> Skolkovo Institute of Science and Technology (Skoltech), 3, Nobel st., Innovation Center Skolkovo, Moscow 121205, Russia; Valentina.Ekimova@skoltech.ru (V.E.); b.bukhanov@skoltech.ru (B.B.); S.Grebenkin@skoltech.ru (S.G.)

<sup>2</sup> National Research Tomsk Polytechnic University, Tomsk Polytechnic University (TPU), 30, Lenin Avenue, Tomsk 634050, Russia; shahova@tpu.ru (N.S.); ipsemiletov@alaska.edu (I.S.)

<sup>3</sup> International Arctic Research Center, University Alaska Fairbanks, 903 Koyukuk Drive, Fairbanks, AK 99775, USA

<sup>4</sup> Pacific Oceanological Institute, Far Eastern Branch of Russian Academy of Sciences, 43, Baltiiskaya st., Vladivostok 690041, Russia

\* Correspondence: e.chuvilin@skoltech.ru

Received: 4 April 2019; Accepted: 20 April 2019; Published: 23 April 2019



**Abstract:** Destabilization of intrapermafrost gas hydrate is one possible reason for methane emission on the Arctic shelf. The formation of these intrapermafrost gas hydrates could occur almost simultaneously with the permafrost sediments due to the occurrence of a hydrate stability zone after sea regression and the subsequent deep cooling and freezing of sediments. The top of the gas hydrate stability zone could exist not only at depths of 200–250 m, but also higher due to local pressure increase in gas-saturated horizons during freezing. Formed at a shallow depth, intrapermafrost gas hydrates could later be preserved and transform into a metastable (relict) state. Under the conditions of submarine permafrost degradation, exactly relict hydrates located above the modern gas hydrate stability zone will, first of all, be involved in the decomposition process caused by negative temperature rising, permafrost thawing, and sediment salinity increasing. That's why special experiments were conducted on the interaction of frozen sandy sediments containing relict methane hydrates with salt solutions of different concentrations at negative temperatures to assess the conditions of intrapermafrost gas hydrates dissociation. Experiments showed that the migration of salts into frozen hydrate-containing sediments activates the decomposition of pore gas hydrates and increase the methane emission. These results allowed for an understanding of the mechanism of massive methane release from bottom sediments of the East Siberian Arctic shelf.

**Keywords:** Arctic shelf; permafrost; gas hydrate; salt migration; thawing; hydrate dissociation; methane emission; environmental impact; geohazards

## 1. Introduction

The Arctic shelf is the most promising hydrocarbon production area. However, its development is associated with the solution of a number of problems that are associated with the conditions of relict permafrost and the presence of gas hydrates [1–4]. Of particular interest is the assessment of methane emissions during the shelf permafrost degradation and the hydrate decomposition due to heat and mass transfer processes. According to many researchers, dissociation of gas hydrate formations in bottom sediments makes the largest contribution to methane emissions on the Arctic shelf [5–12].

Gas hydrates are crystalline clathrate compounds that are formed from gas (mainly methane in natural conditions) and water under certain temperature and pressure conditions [13,14]. An important characteristic of gas hydrates is a huge accumulation of gas in the clathrate structure—up to 160 volumes of gas in one volume of hydrate. As it is well known, methane is one of the most active greenhouse gases. In this regard, the dissociation of Arctic gas hydrates, accompanied by the active emission of methane into the atmosphere, can have a significant greenhouse effect and cause climate change [15,16].

Under natural conditions, gas hydrates are formed and exist in the bottom sediments of the seas and oceans, as well as in the areas of permafrost distribution where there exist favorable temperatures, pressurization, and geochemical conditions. On the Arctic shelf, gas hydrates can be expected at depths of the sea of 250–300 m, as well as at shallower depths in the presence of underwater permafrost. Considering that the thickness of the submarine permafrost can reach several hundred meters, gas hydrate formations can be located both in the sub-permafrost and intrapermafrost horizons [17–20]. The possible existence of hydrates within the gas hydrate stability zone (GHSZ) in the East Siberian Arctic shelf (ESAS) was predicted in the late 1970s, when it was understood that the high-latitude, shallow ESAS has been alternately subaerial and inundated with seawater during glacial and interglacial periods, respectively. Submarine conditions foster the formation of permafrost and associated underlying hydrate deposits, whereas inundation with relatively warm seawater destabilizes the permafrost and hydrates [21,22]. Later, hydrates were found at shallower depths (around 20 m), and their existence within the entire permafrost body was attributed to a so-called “self-preservation phenomenon” [23–25]. These “relict” gas hydrate formations in permafrost soils could have formed earlier, when there were favorable thermobaric conditions. Subsequently, when thermobaric conditions changed, hydrate transferred to the metastable state due to the manifestation of the self-preservation effect [26–29]. Transition from the last glacial period to the current warm Holocene, accompanied by sea level rise that inundated the previously-exposed shelf area, started 5–12 years ago. According to modeling results, sufficient time has elapsed since inundation to cause permafrost/hydrate system destabilization, which is manifested by formation of taliks (areas of completely thawed sediments within a permafrost) in a certain fraction of the ESAS affected by fault zones, runoff from large rivers, and thermokarst [11,18,21,30,31].

ESAS sediments have not been considered a CH<sub>4</sub> source to hydrosphere or atmosphere because submarine permafrost, which underlies most of the ESAS, was considered to be continuous and to act as an impermeable lid [18], preventing CH<sub>4</sub> escape through the seabed. However, multi-year data (2000–2018) showed extreme CH<sub>4</sub> super-saturation of surface waters (up to 10,000% saturation), implying that about 90% of the total ESAS area serves as a source of CH<sub>4</sub> to the atmosphere [12] and high air-to-sea bubble fluxes occur at numerous seepage sites [11,31]. Conservative estimation of CH<sub>4</sub> ebullition from the coastal ESAS areas yields an annual contribution of at least 9 Tg-CH<sub>4</sub>, which increases annual atmospheric flux from the ESAS to 17 Tg-CH<sub>4</sub>, on par with flux from the entire Arctic tundra [11]. That estimate does not include the non-gradual CH<sub>4</sub> release discovered recently on the outer ESAS. Sustained CH<sub>4</sub> release to the atmosphere from thawing Arctic subsea permafrost and dissociating hydrates were suggested to be positive and likely to be significant feedbacks to climate warming [32,33].

Since most hydrate deposits in the Arctic are permafrost-controlled, stability of permafrost is a key to whether hydrates are stable [31]. According to the permafrost thermobaric conditions of the Laptev Sea shelf, there are gas hydrates in the underwater permafrost. However, due to the absence of deep drilling, direct data on the presence of gas hydrate formations is not observed. Nevertheless, by indirect evidence, a number of researchers associate active gas shows with dissociation of gas hydrate formations [12,34–36].

The reason for the hydrate destabilization on the Arctic shelf can be both permafrost degradation as a result of the temperature increase, and the processes of penetration of seawater and salt ions contained in it into the layer of hydrate saturated frozen sediments. Today, the issues of salt transfer as a result of the interaction of cooled sea water with frozen hydrate-containing sediments are not

sufficiently considered. In this regard, the experimental studying of the mechanism and hydrate dissociation parameters in frozen sediments as a result of salt migration is of particular interest for assessing the role of salt transfer in destabilization of intra-permafrost gas hydrate formations and methane emission on the Arctic shelf.

## 2. Methods

Experimental modeling of gas hydrate dissociation in frozen sediments as a result of salt migration included the following steps:

- 1) Preparation of hydrate containing sediment samples, using a pressure cell for artificial hydrate saturation;
- 2) Freezing of hydrate saturated samples in the pressure cell and transfer pore hydrates to a metastable state by reducing gas pressure to atmospheric at a negative temperature;
- 3) Extraction of frozen hydrate-saturated samples from the pressure chamber and their contact with a cooled NaCl solution at constant negative temperature and atmospheric pressure.

The objects of study were sandy samples:

- Quarts fine sand (sand 1)
- Silty sand (predominantly quartz composition) sampling during drilling operations on the Laptev Sea shelf (Buor-Khaya Bay in the area of the Muostakh island) (sand 2) (Table 1), where active gas emission was registered, and according to some indirect data there is a probability of the existence of natural hydrate formations in submarine permafrost [11,16,31,37,38].

**Table 1.** Particle size distribution and mineral composition of investigated sediments.

Sample	Sampling Site	Particle Size Distribution, %						Mineralogy
		1–0.5	0.5–0.25	0.25–0.1	0.1–0.05	0.05–0.001	<0.001	
Sand 1	-	6.5	6.5	79.6	2.2	3.1	2.1	>90% quartz
Sand 2	Laptev Sea shelf (well 1D-11, 40–46 m)	1	9	52	20	16	2	54% quartz 41% microcline + albite 4% illite

The listed mineral phases have percentages >1%.

The initial values of salinity of sandy samples are given in Table 2.

**Table 2.** Salinity and chemical composition of water extracts from investigated sediments.

Sample	Anions, mEq/100 g				Cations, mEq/100 g			Salinity, %
	pH	HCO <sub>3</sub> <sup>-</sup>	Cl <sup>-</sup>	SO <sub>4</sub> <sup>2-</sup>	Ca <sup>2+</sup>	Mg <sup>2+</sup>	Na <sup>+</sup> + K <sup>+</sup>	
Sand 1	7.1	0.075	0.025	0.06	0.025	-	0.135	0.01
Sand 2	8.4	0.89	5.00	-	0.4	4.9	0.6	0.4

The method of obtaining frozen hydrate-containing samples included sediment samples (twins) preparation of a cylindrical shape (about 3 cm in diameter and 6–9 cm long) with a given moisture content (14–16%), and placing them in a pressure cell, sealing and vacuuming the pressure cell with samples, filling the pressure cell by hydrate-forming gas (CH<sub>4</sub>—99.98%), and creation of conditions for uniform saturation of the sediment pore space with gas hydrate [23,39]. Several samples were prepared (about 5–6 pcs.) at the same time, which had similar values of water content, density, and hydrate saturation. After hydrate saturation, which lasted at least 1 month, hydrate saturated sediment samples were frozen at the temperature of  $-7 \pm 1$  °C. As a result, the residual pore moisture in the samples that did not transfer to the hydrate became frozen out. Subsequently, the gas pressure in the cell, which was at a negative temperature, was dropped to 0.1 MPa, converting the frozen pore

hydrate to a metastable state. The frozen hydrate-saturated samples were then taken out. The samples had a massive ice-hydrate texture with pore hydrate contents uniformly distributed over the sample height [23,40].

For the obtained frozen hydrate-containing samples, prior to their contact with the salt solution, the initial physical parameters (moisture content, density, hydrate content) were determined. Then, the hydrate-containing samples were brought into contact and cooled up to the experiment temperature NaCl solution at a temperature below zero. The experiments were carried out at temperatures from  $-2.5\text{ }^{\circ}\text{C}$  to  $-4\text{ }^{\circ}\text{C}$  and concentrations of salt solution from 0.1 to 0.4 N (accordingly to the natural Laptev Sea water concentration, which equals 10–34‰ [41]). The duration of the tests depends on the experimental conditions and ranged from several tens of minutes to several days. For control, one of the samples was stored at a given negative temperature, but was not brought into contact with the salt solution. These control data showed that during the experiment the change in the hydrate content of sediment samples under self-preservation conditions was insignificant, and the main decrease in hydrate saturation of other samples was caused by salt migration.

During the experiments, the dynamics of the interaction of frozen hydrate-containing samples with a salt solution over time, as well as the effect of the concentration of the NaCl contact solution and the ambient temperature on the hydrate dissociation processes in the porous media of sediments were studied. In experimental modeling, hydrate-containing samples were removed from contact solution at certain time intervals. A number of parameters were determined for each sample, characterizing the content of moisture, salts and gas hydrate along the sample length separately in nine-ten 7–10-mm-thick layers of the samples after interaction with the salt solution. This made it possible to trace the dynamics of saline front migration, thawing, and dissociation of gas hydrate formations in frozen sediment samples.

Gas contents were estimated by measuring the volume of gas released (with 2–3 times repeatability) as the samples were thawing in a saturated NaCl solution. Samples with residual hydrate content were put in a special glass tube filled with brine (saline solution), and as a result of gas hydrate dissociation and methane release volume of the brine in the glass tube was changed. And by the volume difference, it was possible to estimate gas content in studied samples. The obtained values were used to estimate hydrate content and hydrate coefficient [23,40], assuming a hydrate number of 5.9 for methane hydrate [19,39,42]. Specific gas content ( $G$ ,  $\text{cm}^3/\text{g}$ ) was found as

$$G = \frac{(V_2 - V_1) * T}{m_s},$$

where:  $(V_2 - V_1)$ —change in the volume of liquid in the gas collector tube ( $\text{cm}^3$ );  $T$ —temperature correction;  $m_s$ —the mass of the sediment sample (g).

The weight gas hydrate content ( $H$ , wt.% of sample weight) was determined for each interval as

$$H = m_g * 7.64 * 100\%, \quad (2)$$

where  $m_g$  is a specific gravity of methane in gas hydrate form (g/g i.e., grams of gas in per gram of sediment) calculated from the specific gas content ( $G$ ) for pure methane.

The fraction of water converted to hydrate or the hydrate coefficient ( $K_h$ , u.f.) is given by

$$K_h = \frac{W_h}{W}, \quad (3)$$

where  $W_h$  is the percentage of water in a hydrate form (wt.% of sample weight) and  $W$  is the total amount of water or moisture content (wt.%) [19,43].

The samples on which the moisture content was determined were further used for the interval determination of the content of salt ions that migrated from the contact salt solution. First of all, water

extractions of salt were made from samples, and then analysis of the  $\text{Na}^+$  ion concentration was carried out by the method of water extracts on a flame photometer PFP-7 (Jenway).

### 3. Results

Experimental modeling showed that the interaction of frozen hydrate saturated sediments with a cooled salt solution leads to an active diffusion of salt ions into the sediment sample, which results in sample salinization. Comparison of experimental data on the accumulation of salt ions in frozen hydrate-containing samples with frozen non-hydrate-containing samples under the same conditions indicates that migration of salt ions in the hydrate-containing samples occurs more intensively. So, in a frozen hydrate-containing sample, 46 h after the start of interaction with a 0.2 N solution of NaCl, ions ( $\text{Na}^+$ ) penetrated 7.3 cm deep into the sample, and in a frozen non-hydrate-containing sample, only 5.6 cm deep with higher salt accumulation (Figure 1).

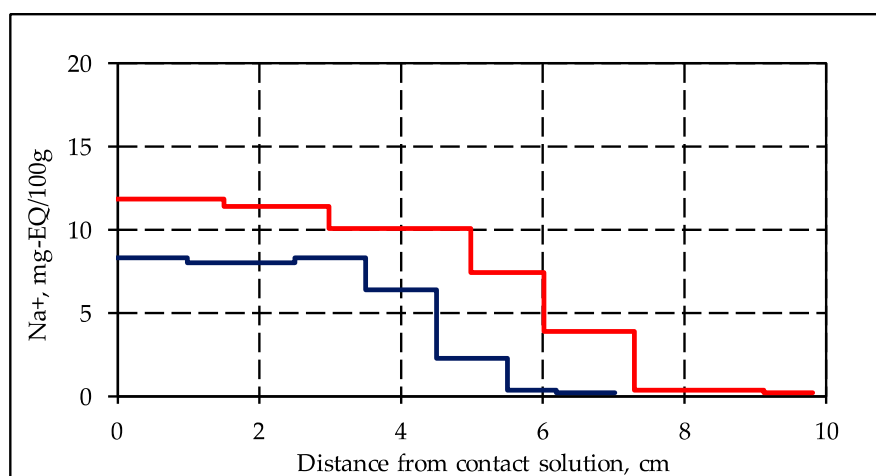


**Figure 1.** Salt ion accumulations ( $\text{Na}^+$ ) in frozen sand samples (sand 1,  $W = 14\%$ ) containing (red line) and not containing (blue line) hydrate in porous media after 46 h of contact with 0.2N NaCl solution under the temperature  $-4\text{ }^\circ\text{C}$ .

The process of migration of salt ions in the frozen hydrate-containing sample was accompanied by an increase in the liquid phase content in the sample and hydrate dissociation in the pore space.

Migrating salt ions cause melting of ice in porous media, including ice on the surface of conserved gas hydrates in the pore space of the frozen sample, and thereby activate the gas hydrate decomposition. Experimental studies allowed us to trace the movement in time of the salinity front of the frozen hydrate-containing sample under negative temperature conditions ( $-4\text{ }^\circ\text{C}$ ) (Figure 2). After 4 h of frozen hydrate-containing sample contact with a salt solution, the salt ions ( $\text{Na}^+$ ) penetrated on 2.5 cm, the salt ion content in the contact zone increased up to 0.7 mg EQ/ 100 g, and a day later (29 h after the start of the experiment) salts penetrated to a depth of about 5 cm. The maximum accumulation of salt ions in the sample reached 1.6 mg EQ/ 100 g.

The accumulation of salt ions in the studied sand samples affected the hydrate content. In the initial state (before contact with the solution) for sand samples (sand 1) about 60% of the pore moisture was in the hydrate form, while the hydrate saturation of the samples was about 40%. In the process of unilateral salinization, the proportion of pore moisture in the hydrate form ( $K_h$ ) decreased, and the front of the complete decomposition of the gas hydrate appeared (Figure 3).

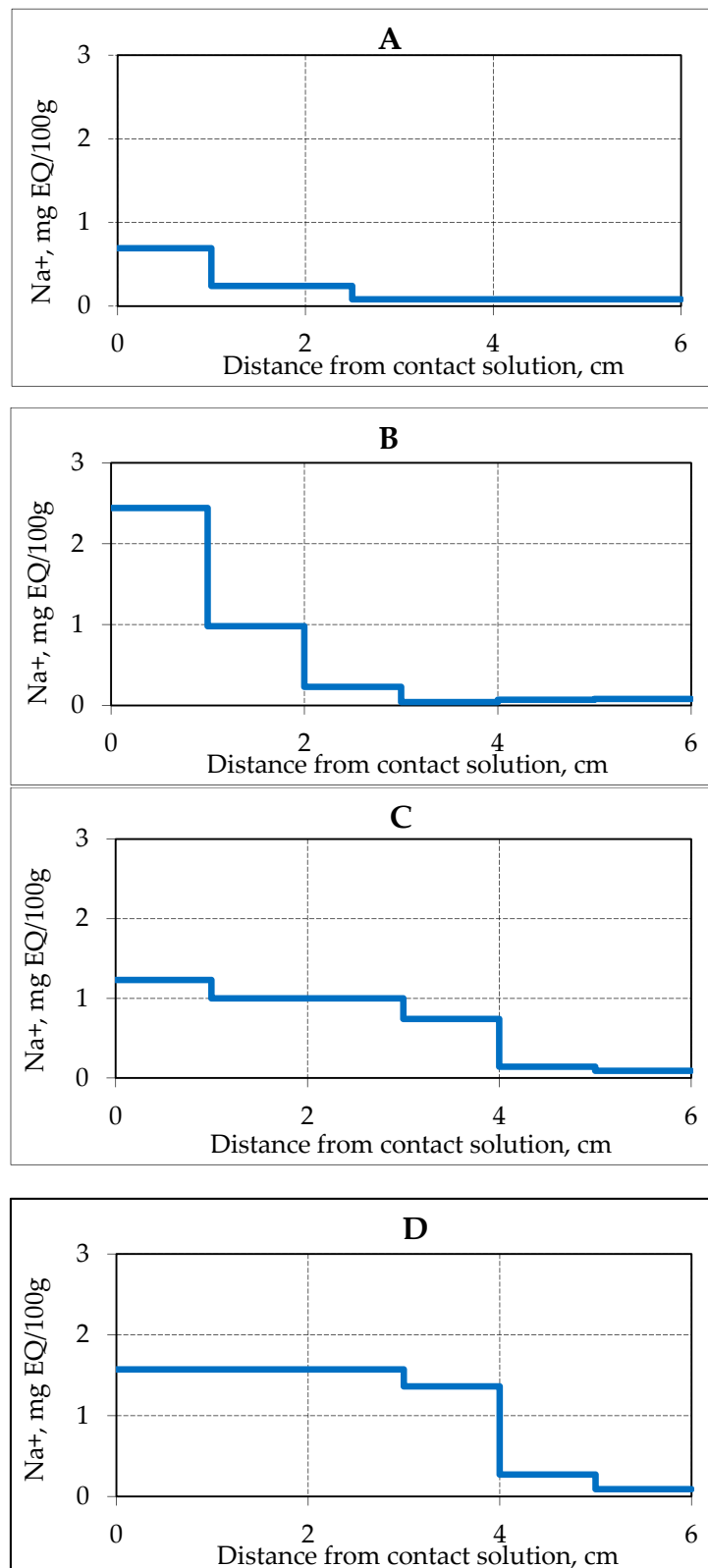


**Figure 2.** Accumulation of Na<sup>+</sup> ions in samples of frozen hydrate saturated sand (sand 1, W = 14%) in time when interacting with 0.2 N NaCl solution at a temperature of −4 °C. (A–D) is the time of interaction with the salt solution, respectively, 3.9, 17.5, 25.5 and 28.8 h.

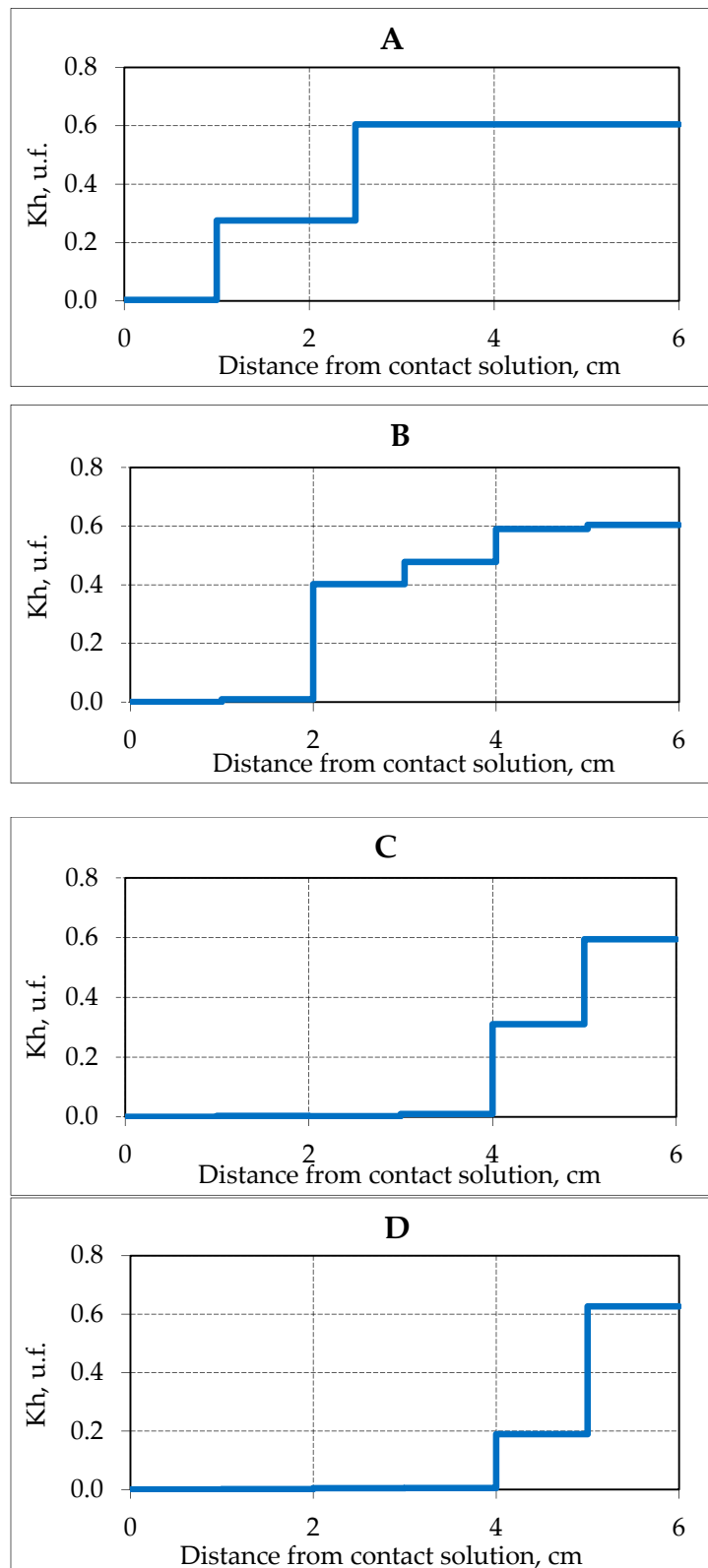


**Figure 3.** The change in the hydration coefficient ( $K_h$ ) in frozen hydrate saturated samples of sand (sand 1,  $W = 14\%$ ) in time when interacting with 0.2 N NaCl salt solution at a temperature of  $-4\text{ }^\circ\text{C}$ . (A–D) is the time of interaction with the salt solution, respectively, 3.9, 17.5, 25.5 and 28.8 h.

A joint analysis of the distribution of salt ions (Figure 2) and the hydration coefficient ( $K_h$ ) over the height of the sample (Figure 3) shows that the amount of salinity determines the residual content of



pore gas hydrate. In this case, it is possible to determine a certain critical content of salt ions in sandy samples, which causes the complete decomposition of gas hydrate formations in the sediment. Under specified conditions (temperature  $-4\text{ }^{\circ}\text{C}$  and the concentration of a contact solution of NaCl 0.2 N) in sediment samples (sand 1), the critical salt accumulation was about 0.7–0.8 mg EQ/ 100 g.

In the process of salts migration in the frozen hydrate-containing sample, in addition to the hydrate decomposition front in porous media, a thawing front may occur when the accumulated salt ions completely transform pore ice into water. The movement of two fronts can be traced on Figure 4: hydrate decomposition front and thawing of pore ice.

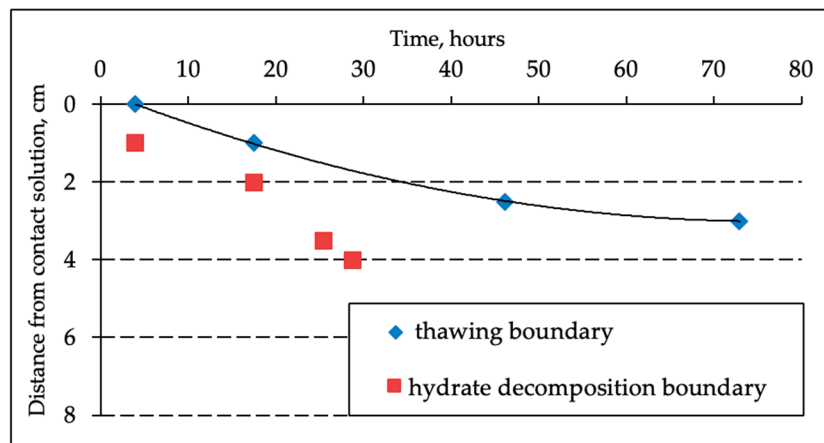


**Figure 4.** Experimental assessment of the gas hydrate decomposition front in porous media and the thawing front in frozen hydrate-containing sandy samples (sand-1,  $W = 14\%$ ) when interacting with 0.2 N NaCl salt solution at the temperature  $-4\text{ }^{\circ}\text{C}$ .

The hydrate decomposition front is ahead of the thawing front since a higher value of salt accumulation in the frozen sample is needed for thawing. The thawing front in the sample is well marked by the characteristic change in the color of the sample (Figure 5). Additionally, it was evaluated using a special needle probe.



**Figure 5.** Frozen sandy samples (sand 2,  $W = 15\%$ ) before (A) and after interaction (B) with 0.2 N NaCl solution at  $-3\text{ }^{\circ}\text{C}$ .

With an increase in the ambient temperature, the processes of salinity migration of the frozen hydrate-containing sediment, and, consequently, the gas hydrate decomposition rate in pore space increase. The study of the interaction dynamics of frozen hydrate saturated sediment (sand 2) with 0.2 N NaCl solution at the conditions of negative temperature increase (up to  $-2.5\text{ }^{\circ}\text{C}$ ) showed that



the penetration rate of salt ions rises significantly. At a higher negative temperature, the NaCl ions penetrated deeper in a shorter time (Figure 6).

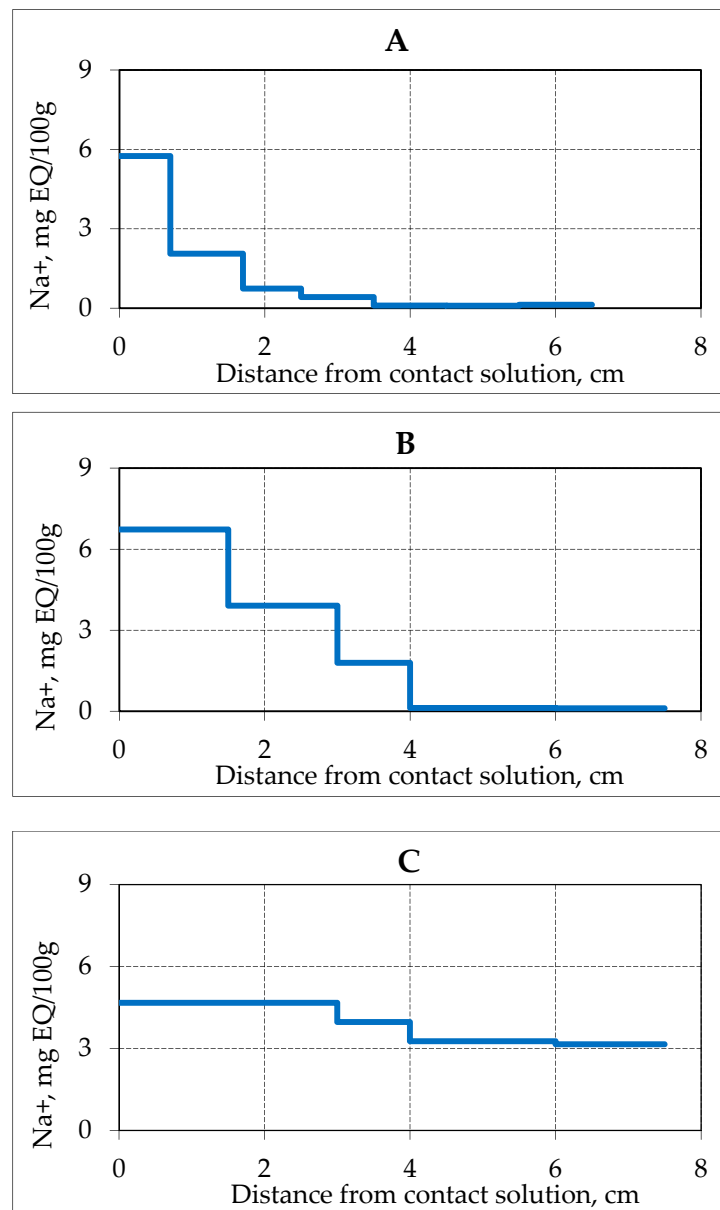


**Figure 6.** Accumulation of Na<sup>+</sup> ions in samples of frozen hydrate saturated sand (sand 2, W = 16%) over time when interacting with 0.2 N NaCl solution at a temperature −2.5 °C. (A–C)—the time of interaction with salt solution, respectively, 0.3, 0.9 and 2.6 h.

So, already 1 h after the experiment start, salt ions penetrated on a distance of 4 cm from the salt solution contact zone, and after 2.6 h, the migrating salt ions were registered along the entire length of the sample (about 7 cm). An increase in the moisture content of the sample due to the migrating solution was also observed. At the beginning of the experiment (0.3 h), the increase in water content was only in the contact zone, and at the end of the experiment (2.6 h) along the entire length of the sample. The overall increase in moisture content occurred from 16 to 30%, and in the contact area up to 50%. The concentration of ions (Na<sup>+</sup>) was about 5 mg EQ/100 g in the contact area at the end of the experiment, which is more than 3 times the maximum concentration of salt ions in the experiment at a lower negative temperature (−4 °C). More intensive migration of NaCl solution in frozen hydrate

saturated sediments at a temperature of  $-2.5\text{ }^{\circ}\text{C}$  cause more active gas hydrate decomposition in pore space (Figure 7).

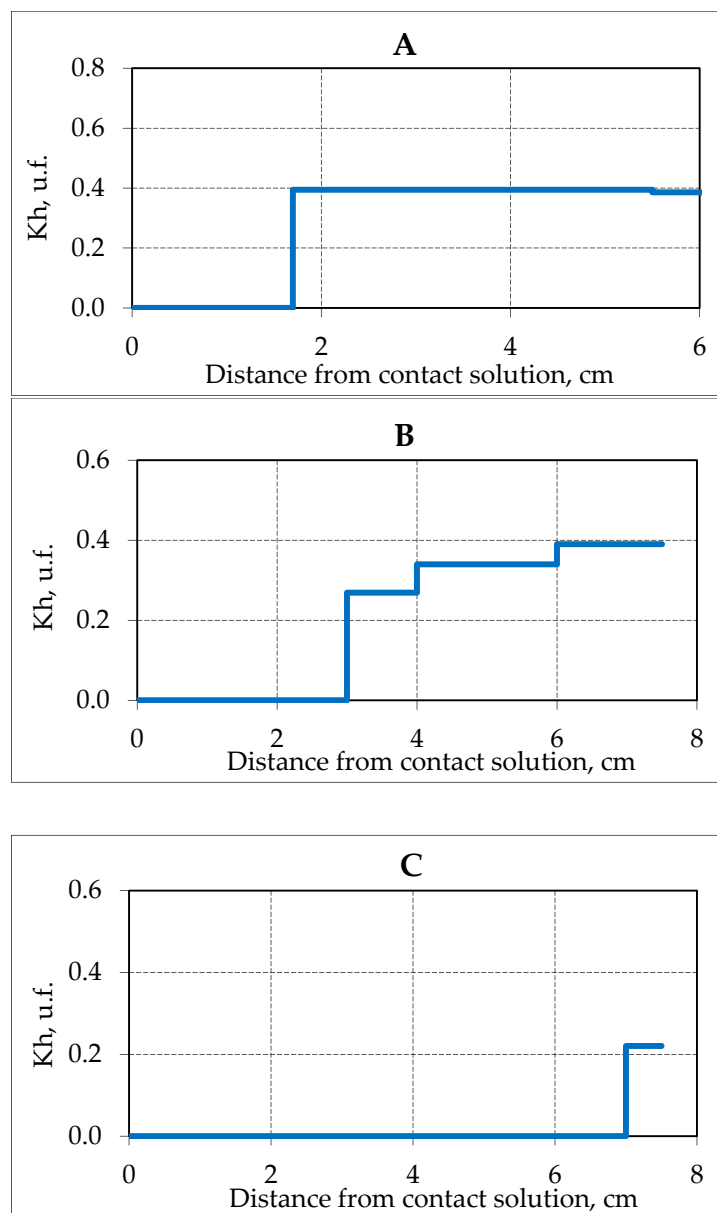


**Figure 7.** The change in the hydration coefficient ( $K_h$ ) in samples of frozen hydrate saturated sand (sand 2,  $W = 16\%$ ) in time when interacting with 0.2 N NaCl solution at a temperature of  $-2.5\text{ }^{\circ}\text{C}$ . (A–C) is the time of interaction with the salt solution, respectively, 0.3; 0.9; 2.6 h.

Before the contact of the frozen hydrate-containing sample (sand 2) with a salt solution, about 40% of the pore moisture was in the gas hydrate form. After 0.3 h, from the beginning of the contact of frozen hydrate-containing sample with the salt solution at  $-2.5\text{ }^{\circ}\text{C}$ , the pore hydrate completely decomposed at a distance of 1.8 cm from the contact area, after 0.9 h—at a distance of 3 cm, and after 2.6 h—7 cm. At the time of the experiment end, the residual values of  $K_h$  (about 25%) were registered only in a narrow zone of the sample at the sample opposite end from the contact.

An increase in the concentration of a saline solution in contact with a frozen hydrate-containing sample at a fixed negative temperature also leads to more intense gas hydrate dissociation in porous media, an increase in the rate of movement of the salinity fronts and gas hydrate decomposition. For example, at a fixed interaction time (3 h) of a frozen hydrate saturated sample (sand 2) at a

temperature of  $-3\text{ }^{\circ}\text{C}$  with a saline solution 0.1 N salt ions ( $\text{Na}^+$ ) migrated to a depth of 1.8 cm, and at a concentration of contacting solution 0.4 N salt ions migrated almost over the entire length of the sample. The content of salt ions in the contact area of the sample with an increase in the concentration of the contacting solution (from 0.1N to 0.4 N) increased 6 times in 3 h of the experiment (Figure 8).

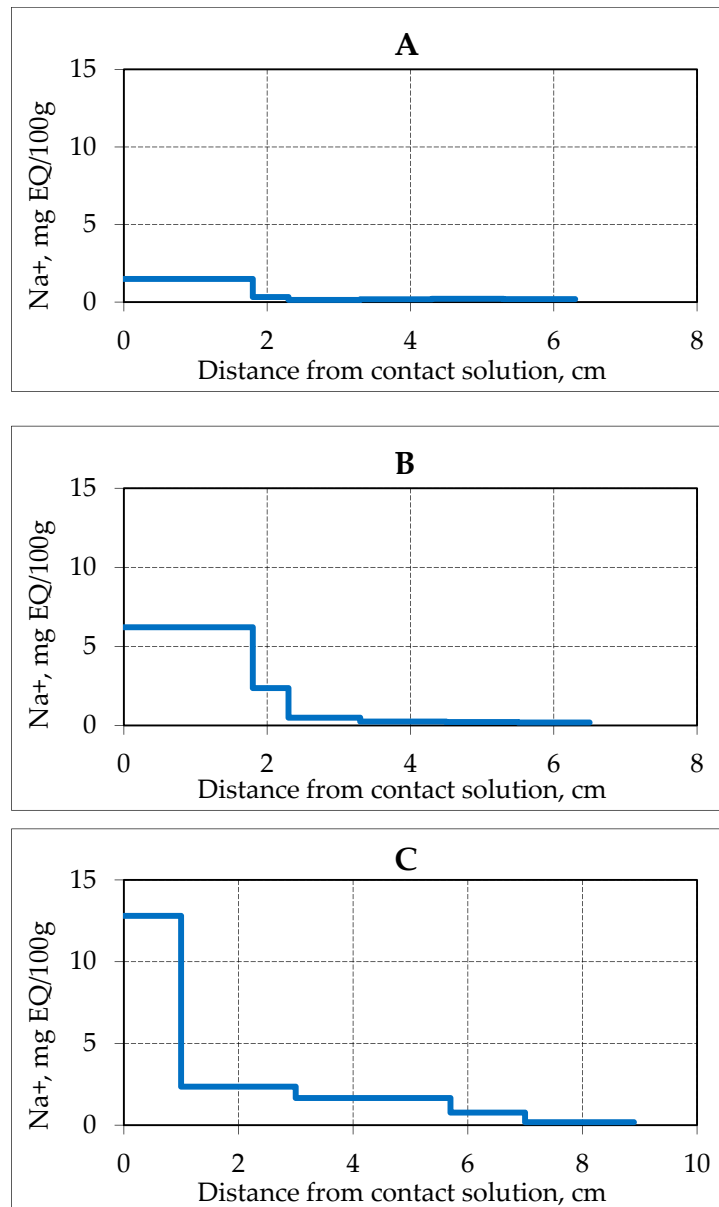


**Figure 8.** Accumulation of  $\text{Na}^+$  ions in samples of frozen hydrate saturated sand (sand 2,  $W = 16\%$ ) after 3 h of contact with NaCl solution of various concentrations at a temperature of  $-3\text{ }^{\circ}\text{C}$ . (A–C)—solution concentration, respectively, 0.1, 0.2 and 0.4 N.

At the same time, an increase in the moisture content of the sample from 16% to 60% was recorded in the contact zone.

An increase in the concentration of the contact solution accelerated movement of the gas hydrate dissociation front in the porous space of the frozen hydrate saturated sample. Thus, at a concentration of a contact solution of 0.1 N NaCl, the complete decomposition of a pore gas hydrate in a sediment sample occurred at a distance of 1.9 cm, and at a concentration of 0.4 N, the pore gas hydrate completely dissociated at a distance of 3 cm from the contact area. The maximum value of  $K_h$  in the samples

decreased with an increase in the concentration of the contact solution from 26% to a residual value of 17% after the experiment (Figure 9).

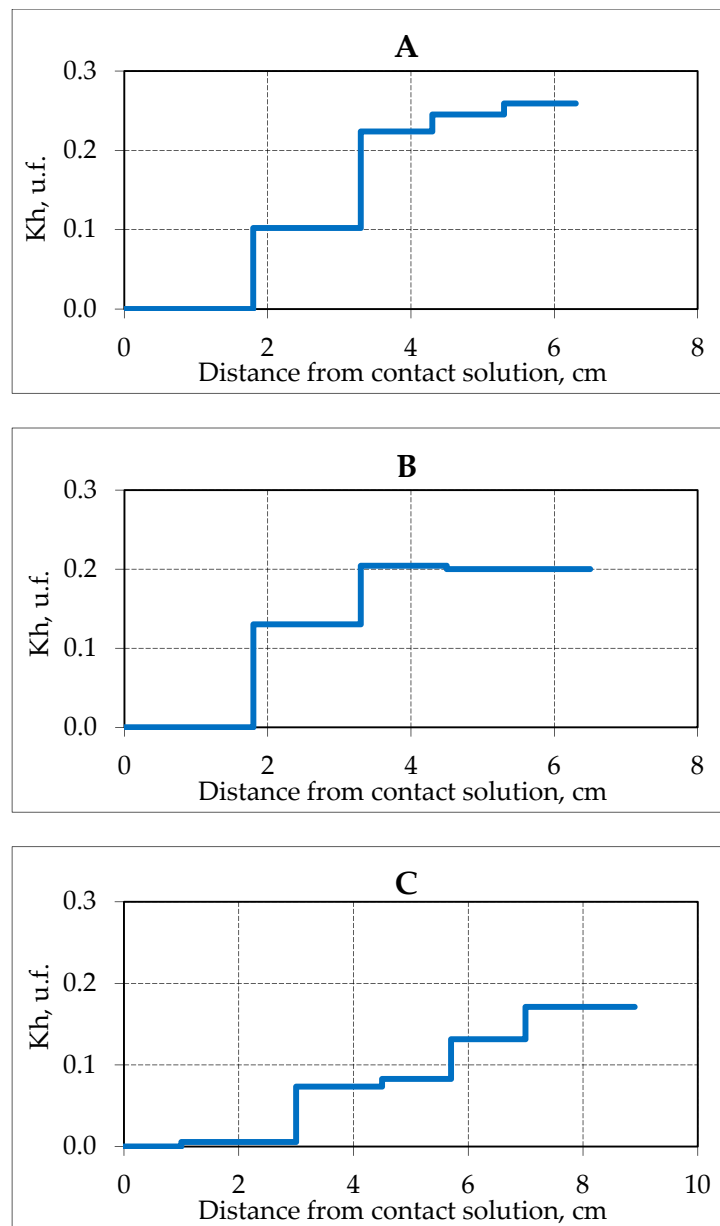


**Figure 9.** Changes in the hydration coefficient ( $K_h$ ) in samples of frozen hydrate saturated sand (sand 2,  $W = 16\%$ ) after 3 h of contact with NaCl solution of various concentrations at a temperature of  $-3\text{ }^\circ\text{C}$ . (A–C) solution concentration, respectively, 0.1, 0.2 and 0.4 N.

Data on the change in hydrate content of frozen hydrate-saturated sediments when interacting with a saline solution were used to estimate the kinetics of methane emission from frozen samples during decomposition of pore gas hydrates depending on temperature (Figure 10).

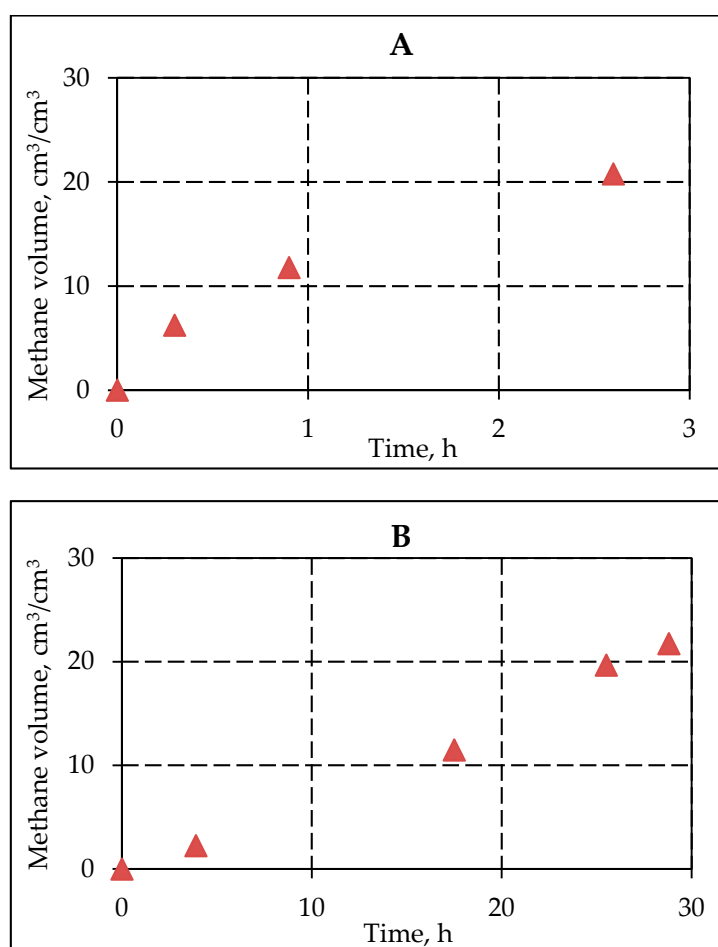


**Figure 10.** Methane emission in frozen hydrate saturated samples of sand (sand 1) during the gas hydrate dissociation in the pore space as a result of interaction with 0.2 N NaCl salt solution at temperatures  $-2.5\text{ }^{\circ}\text{C}$  (A) and  $-4\text{ }^{\circ}\text{C}$  (B).

The calculated data show that the intensity of methane release from frozen hydrate-containing samples depends on the salt ions migration rate. The more intense accumulation of salt ions at a higher negative temperature of  $-2.5\text{ }^{\circ}\text{C}$  led to the fact that the relative emission of methane exceeded  $10\text{ cm}^3/\text{cm}^3$  just one hour after the start of interaction with the salt solution.

Experimental results demonstrated active salt migration in frozen hydrate saturated sediment while interacting with salt solutions, which leads to thawing of frozen sediment, destruction of intrapermafrost gas hydrate formations and methane emission.

#### 4. Discussion

One of the possible causes of the decomposition of intrapermafrost gas hydrates on the Arctic shelf may be the migration of salt ions as a result of sea water interaction with underwater permafrost. At present, there are practically no special studies in the literature on the gas hydrate dissociation in frozen sediments porous media as a result of salt transfer. Although they may be important for understanding the nature of methane emissions during the degradation of permafrost on the Arctic shelf. However, since the 1980s it has been known that the interaction of frozen sediments with salt solutions leads to the active migration of salt ions [44–46]. In this case, several mechanisms for the salt ions transfer in frozen sediment were described, and also some regularities of their transfer depending on external conditions were considered. In general, it was shown that the transfer of salt ions in frozen sediment is primarily determined by the characteristics of the sediment itself (dispersion, chemical and mineral composition, ice content), as well as temperature conditions and the

concentration of salt solutions, and is accompanied by the processes of moisture transfer and structure formation [45,47,48]. The experimental data on the interaction of frozen hydrate saturated sediments with salt solutions showed that the migration of salt ions in frozen hydrate-containing sediment can occur more intensively compared to frozen rocks non-containing hydrates, which is apparently due to the process of dissociation of the pore hydrate and the appearance of this liquid phase water. With an increase in the temperature of frozen hydrate bearing sediments and salt concentrations, the intensity of mass transfer processes increases. In this case, two fronts are observed: the hydrate decomposition front and the thawing front. The front of the hydrate dissociation in pore space is ahead of the thawing boundary, since the phase transition of pore ice into water requires higher accumulations of salt ions during their migration.

Schematic diagram presenting current understanding of the subsea permafrost – hydrate system existing in the ESAS is presented and discussed by [49]. Below we focus on the salt/hydrates effect which was not studied experimentally before. Our new experimental data can be used to illustrate interaction between cold bottom sea water and cold/thaw sediments/subsea permafrost, and hydrates. Downward salt migration can be considered a factor of relic hydrates dissociation (Figure 11).

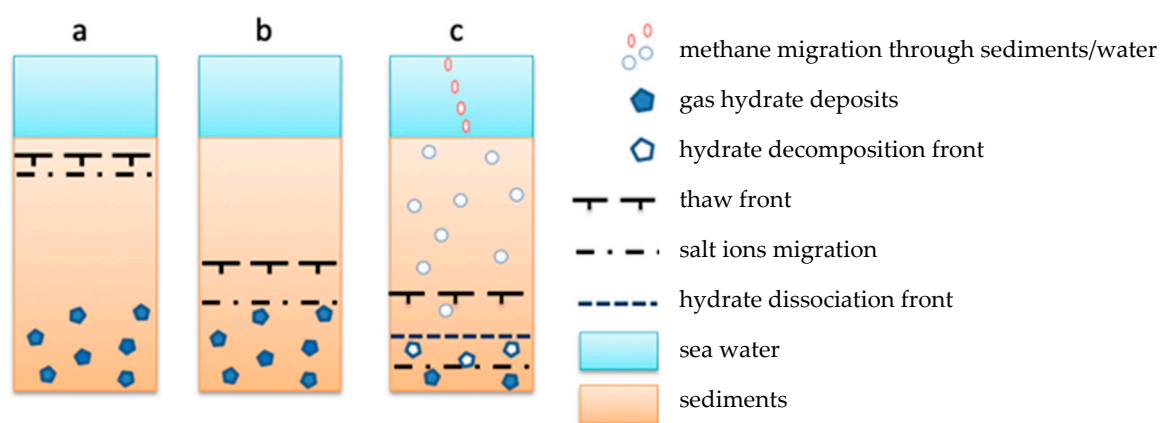


**Figure 11.** An estimated model of the interaction of cooled sea water with frozen sediments containing relict gas hydrates. (a) Initial state (interaction between cold seawater and frozen sediments); (b) Penetration of sea salt into permafrost (formation of salinity and thawing fronts); (c) Interaction of salt front with intra-permafrost gas hydrate accumulations (decomposition of gas hydrates, active methane emissions).

At the initial stage (Figure 11a), and after the transgression of the Arctic Sea, there is an active interaction of seawater with underlying frozen sediment, resulting in a change in the permafrost temperature and the formation of a thawing front [31]. Over time, the rate of thawing of the underwater permafrost decreases. At the same time, the penetration of seawater into the thawing zone is identified (Figure 11b). Since the frozen rocks are permeable to salt ions, the advance movement of salt ions from seawater relative to the thawing front is observed. During migration and accumulation of salt ions in frozen sediments, a decrease in the temperature of phase transitions and an increase in the content of the liquid phase in sediments occurs. As a result, deceleration rate of thawing front decreases. Salt ions migrating in frozen sediments upon reaching horizons containing relict hydrates will destabilize them and promote their active dissociation and release of methane (Figure 11c), thus forming the second phase transition phase—the front of gas hydrate dissociation. It occurs when a certain critical salt concentration is reached in the frozen hydrate-containing rock. This concentration, as shown by experimental studies, depends on the composition of hydrate-containing sediments and thermobaric conditions. During phase transitions (hydrate-ice-water) caused by salt migration the gas permeability of salted frozen sediments increases [50]. Methane formed during the dissociation of gas hydrates further migrates to the bottom surface and enters seawater, where it is partially dissolved, oxidized, and also diffused through the water column before it goes into the atmosphere (Figure 11c). The

detailed explanation of the methane upward transport in the sediment-water column-atmosphere system can be found in [49].

This scheme makes it possible to explain the possible cause of the numerous gas manifestations recorded on the Arctic shelf in the areas of distribution of submarine permafrost as a result of the destabilization of the permafrost gas hydrate formations due to heat and mass transfer processes associated with the migration of salt ions from seawater.

## 5. Conclusions

New experimental results integrated with the observational data confirm a hypothesis about the primary role of submarine permafrost and hydrate destabilization in a massive methane release in the sediment-water-atmosphere system [11,12,31,49]. As a result of the degradation of relic submarine permafrost (containing hydrates), active dissociation of intrapermafrost gas hydrate can occur. As shown by experimental modeling, salt transfer plays an important role in this process.

Experimental studies revealed that salt migration during the interaction of frozen hydrate saturated sediments with salt solutions causes their migration through frozen horizons, which leads to decomposition of intrapermafrost gas hydrates and permafrost thawing. It was experimentally shown that in the process of salts transfer and accumulation, two fronts are formed: thawing of frozen sediments and gas hydrate decomposition. It is noted that the front of decomposition of gas hydrate is ahead of the front of thawing.

Experimental studies allowed us to trace the dynamics of the thawing front and the decomposition front of gas hydrates, caused by the migration of salts in frozen hydrate-containing sediments, and also to obtain some consistencies on the hydrate dissociation in pore space in frozen sediments depending on the ambient temperature and the salt solution concentration. According to the experimental modeling, methane emissions were estimated during the decomposition of pore gas hydrates in frozen sediments during salt transfer. The results of the experiments were used to build a model of the interaction of the hydrate saturated permafrost with sea water on the Arctic shelf.

**Author Contributions:** Conceptualization, E.C.; sampling, B.B., S.G.; experimental methodology, E.C., V.E., B.B. and S.G.; calculation methodology, E.C., V.E.; experiments, processing, and analysis, E.C., V.E. and B.B.; supervision, E.C., I.S.; writing manuscript and editing, E.C., V.E., B.B., N.S. and I.S.

**Funding:** The research was supported partly by the Russian Science Foundation (grants No. 16-17-00051, 18-77-10063 and 15-17-20032).

**Conflicts of Interest:** The authors declare no conflict of interest.

## References

1. Yakushev, V.S.; Collett, T.S. Gas Hydrates in Arctic Regions: Risk to Drilling and Production. In Proceedings of the Second International Offshore and Polar Engineering Conference, San Francisco, CA, USA, 14–19 June 1992; Volume 1, pp. 669–673. [\[CrossRef\]](#)
2. Safronov, A.F.; Shits, E.Y.; Grigor'ev, M.N.; Semenov, M.E. Formation of Gas Hydrate Deposits in the Siberian Arctic Shelf. *Russ. Geol. Geophys.* **2010**, *51*, 83–87. [\[CrossRef\]](#)
3. Paull, C.K.; Ussler, W.; Dallimore, S.R.; Blasco, S.M.; Lorenson, T.D.; Melling, H.; Medioli, B.E.; Nixon, F.M.; McLaughlin, F.A. Origin of Pingo-like Features on the Beaufort Sea Shelf and Their Possible Relationship to Decomposing Methane Gas Hydrates. *Geophys. Res. Lett.* **2007**, *34*, L01603:1–L01603:5. [\[CrossRef\]](#)
4. Romanovskii, N.N.; Hubberten, H.W.; Gavrilov, A.V.; Eliseeva, A.A.; Tipenko, G.S.; Kholodov, A.L.; Romanovsky, V.E. Permafrost and Gas Hydrate Stability Zone Evolution on the Eastern Part of the Eurasia Arctic Sea Shelf in the Middle Pleistocene-Holocene (Published in Russian). *Earth's Cryosph.* **2003**, *7*, 51–64.
5. Andreassen, K.; Hubbard, A.; Winsborrow, M.; Patton, H.; Vadakkepuliambatta, S.; Plaza-faverola, A.; Deryabin, A.; Mattingsdal, R.; Mienert, J. Gas Hydrate Regulate Methane Emissions from Arctic Petroleum Basins. In Proceedings of the 9th International Conference on Gas Hydrates (ICGH9), Denver, CO, USA, 25–30 June 2017; p. 2.



6. Mau, S.; Romer, M.; Torres, M.E.; Bussmann, I.; Pape, T.; Damm, E.; Geprags, P.; Wintersteller, P.; Hsu, C.W.; Loher, M.; et al. Widespread Methane Seepage along the Continental Margin off Svalbard—From Bjornoya to Kongsfjorden. *Sci. Rep.* **2017**, *7*, 42997:1–42997:13. [CrossRef]
7. Wood, W.T.; Gettrust, J.F.; Chapman, N.R.; Spence, G.D.; Hyndman, R.D. Decreased Stability of Methane Hydrates in Marine Sediments Owing to Phase-Boundary Roughness. *Nature* **2002**, *420*, 656–660. [CrossRef]
8. Serov, P.; Vadakkepuliyambatta, S.; Mienert, J.; Patton, H.; Portnov, A.; Silyakova, A.; Panieri, G.; Carroll, M.L.; Carroll, J.; Andreassen, K.; et al. Postglacial Response of Arctic Ocean Gas Hydrates to Climatic Amelioration. *Proc. Natl. Acad. Sci. USA* **2017**, *114*, 6215–6220. [CrossRef] [PubMed]
9. Dean, J.F.; Middelburg, J.J.; Röckmann, T.; Aerts, R.; Blauw, L.G.; Egger, M.; Jetten, M.S.M.; de Jong, A.E.E.; Meisel, O.H.; Rasigraf, O.; et al. Methane Feedbacks to the Global Climate System in a Warmer World. *Rev. Geophys.* **2018**, *56*, 207–250. [CrossRef]
10. James, R.H.; Bousquet, P.; Bussmann, I.; Haeckel, M.; Kipfer, R.; Leifer, I.; Niemann, H.; Ostrovsky, I.; Piskozub, J.; Rehder, G.; et al. Effects of Climate Change on Methane Emissions from Seafloor Sediments in the Arctic Ocean: A Review. *Limnol. Oceanogr.* **2016**, S283–S299. [CrossRef]
11. Shakhova, N.; Semiletov, I.; Leifer, I.; Sergienko, V.; Salyuk, A.; Kosmach, D.; Chernykh, D.; Stubbs, C.; Nicolsky, D.; Tumskey, V.; et al. Ebullition and Storm-Induced Methane Release from the East Siberian Arctic Shelf. *Nat. Geosci.* **2014**, *7*, 64–70. [CrossRef]
12. Shakhova, N.; Semiletov, I.; Salyuk, A.; Yusupov, V.; Kosmach, D.; Gustafsson, Ö. Extensive Methane Venting to the Atmosphere from Sediments of the East Siberian Arctic Shelf. *Science* **2010**, *327*, 1246–1250. [CrossRef]
13. Makogon, Y.F. *Hydrates of Natural Gas (Published in Russian)*; Nedra: Moscow, Russia, 1974; p. 208. ISBN 978-364-214-233-8.
14. Max, M. *Natural Gas Hydrate in Oceanic and Permafrost Environments*; Kluwer Academic Publishers: Washington, DC, USA, 2000; ISBN 978-1-4020-1362-1. [CrossRef]
15. Shakhova, N.E.; Alekseev, V.A.; Semiletov, I.P. Erratum to: “Predicted Methane Emission on the East Siberian Shelf.” *Dokl. Earth Sci.* **2013**, *452*, 1074. [CrossRef]
16. Sergienko, V.I.; Lobkovskii, L.I.; Semiletov, I.P.; Dudarev, O.V.; Dmitrievskii, N.N.; Shakhova, N.E.; Romanovskii, N.N.; Kosmach, D.A.; Nikol’skii, D.N.; Nikiforov, S.L.; et al. The Degradation of Submarine Permafrost and the Destruction of Hydrates on the Shelf of East Arctic Seas as a Potential Cause of the “Methane Catastrophe”: Some Results of Integrated Studies in 2011. *Dokl. Earth Sci.* **2012**, *446*, 1132–1137. [CrossRef]
17. Solov’yev, V.A.; Ginsburg, G.D. Formation of Submarine Gas Hydrates. *Bull. Geol. Soc. Den.* **1994**, *41*, 86–94.
18. Romanovskii, N.N.; Hubberten, H.-W.; Gavrillov, A.V.; Eliseeva, A.A.; Tipenko, G.S. Offshore Permafrost and Gas Hydrate Stability Zone on the Shelf of East Siberian Seas. *Geo-Mar. Lett.* **2005**, *25*, 167–182. [CrossRef]
19. Chuvilin, E.; Davletshina, D. Formation and Accumulation of Pore Methane Hydrates in Permafrost: Experimental Modeling. *Geosciences* **2018**, *8*, 467. [CrossRef]
20. Yakushev, V.S. *Natural Gas and Gas Hydrates in the Permafrost (Published in Russian)*; Gazprom VNIIGAZ: Moscow, Russia, 2009; p. 192.
21. Solov’ev, V.A.; Ginsburg, G.D. *Submarine Gas Hydrates (Published in Russian)*; VNII Oceanologii: St. Petersburg, Russia, 1994; ISBN 5-7173-0290-8.
22. Solov’ev, V. A Global Estimate of the Amount of Gas in Submarine Accumulations of Gas Hydrates. *Geol. Geophys.* **2002**, *43*, 648–661.
23. Chuvilin, E.; Bukhanov, B.; Davletshina, D.; Grebenkin, S.; Istomin, V. Dissociation and Self-Preservation of Gas Hydrates in Permafrost. *Geosciences* **2018**, *8*, 431. [CrossRef]
24. Yakushev, V.S. Gas Hydrates in Cryolithozone (Published in Russian). *Sov. Geol. Geophys.* **1989**, *1*, 100–105.
25. Chuvilin, E.M.; Yakushev, V.S.; Perlova, E.V. Gas and Possible Gas Hydrates in the Permafrost of Bovanenkovo Gas Field, Yamal Peninsula, West Siberia. *Polarforschung* **2000**, *68*, 215–219.
26. Hachikubo, A.; Takeya, S.; Chuvilin, E.; Istomin, V. Preservation Phenomena of Methane Hydrate in Pore Spaces. *Phys. Chem. Chem. Phys.* **2011**, *13*, 17449–17452. [CrossRef]
27. Istomin, V.; Yakushev, V.; Makhonina, N.; Kwon, V.G.; Chuvilin, E.M. Self-Preservation Phenomenon of Gas Hydrate (Published in Russian). *Gas Ind.* **2006**, 36–46. Available online: <https://istina.msu.ru/publications/article/2428015/> (accessed on 23 April 2019).
28. Takeya, S.; Ebinuma, T.; Uchida, T.; Nagao, J.; Narita, H. Self-Preservation Effect and Dissociation Rates of CH<sub>4</sub> Hydrate. *J. Cryst. Growth* **2002**, *237*, 379–382. [CrossRef]

29. Ershov, E.D.; Lebedenko, Y.P.; Chuvilin, E.M.; Istomin, V.A.; Yakushev, V.S. Features of the Existence of Gas Hydrates in the Cryolithozone (Published in Russian). *Rep. Acad. Sci. USSR* **1991**, *321*, 788–791.
30. Nicolsky, D.; Shakhova, N. Modeling Sub-Sea Permafrost in the East Siberian Arctic Shelf: The Dmitry Laptev Strait. *Environ. Res. Lett.* **2010**, *5*, 015006:1–015006:9. [[CrossRef](#)]
31. Shakhova, N.; Semiletov, I.; Gustafsson, O.; Sergienko, V.; Lobkovsky, L.; Dudarev, O.; Tumskey, V.; Grigoriev, M.; Chernykh, D.; Koshurnikov, A.; et al. Current Rates and Mechanisms of Subsea Permafrost Degradation in the East Siberian Arctic Shelf. *Nat. Commun.* **2017**, *8*, 15872:1–15872:13. [[CrossRef](#)]
32. ACIA. *Future Climate Change: Modeling and Scenarios*; Cambridge University Press: Cambridge, UK, 2005; pp. 99–150.
33. Westbrook, G.K.; Thatcher, K.E.; Rohling, E.J.; Piotrowski, A.M.; Pälike, H.; Osborne, A.H.; Nisbet, E.G.; Minshull, T.A.; Lanoisellé, M.; James, R.H.; et al. Escape of Methane Gas from the Seabed along the West Spitsbergen Continental Margin. *Geophys. Res. Lett.* **2009**, *36*, L15608:1–L15608:5. [[CrossRef](#)]
34. Nicolsky, D.J.; Romanovsky, V.E.; Romanovskii, N.N.; Kholodov, A.L.; Shakhova, N.E.; Semiletov, I.P. Modeling Sub-Sea Permafrost in the East Siberian Arctic Shelf: The Laptev Sea Region. *J. Geophys. Res. Earth Surf.* **2012**, *117*, F03028:1–F03028:22. [[CrossRef](#)]
35. Delisle, G. Temporal Variability of Subsea Permafrost and Gas Hydrate Occurrences as Function of Climate Change in the Laptev Sea, Siberia. *Polarforschung* **2000**, *68*, 221–225.
36. Romanovskii, N.N.; Eliseeva, A.A.; Gavrilov, A.V.; Tipenko, G.S.; Hubberten, X. The Long-Term Dynamics of Frozen Strata and the Zone of Gas Hydrate Stability in the Rift Structures of the Arctic Shelf of Eastern Siberia (Report 2) (Published in Russian). *Earth's Cryosph.* **2006**, *10*, 29–38.
37. Chuvilin, E.M.; Tumskey, V.E.; Tipenko, G.S.; Gavrilov, A.V.; Bukhanov, B.A.; Tkacheva, E.V.; Audibert-Hayet, A.; Cauquil, E. Relic Gas Hydrate and Possibility of Their Existence in Permafrost within the South-Tambey Gas Field. In Proceedings of the SPE Arctic and Extreme Environments Technical Conference and Exhibition, Moscow, Russia, 15–17 October 2013; pp. 166925:1–166925:9.
38. Chuvilin, E.; Bukhanov, B.; Grebenkin, S.; Tumskey, V.; Shakhova, N.; Dudarev, O.; Semiletov, I. Thermal Conductivity of Bottom Sediments in the East Siberian Arctic Seas: A Case Study in the Buor-Khaya Bay. In Proceedings of the 7th Canadian Permafrost Conference, Québec City, QC, Canada, 21–23 September 2015; pp. ABS557:1–ABS557:6.
39. Chuvilin, E.; Bukhanov, B. Thermal Conductivity of Frozen Sediments Containing Self-Preserved Pore Gas Hydrates at Atmospheric Pressure: An Experimental Study. *Geosciences* **2019**, *9*, 65. [[CrossRef](#)]
40. Chuvilin, E.M.; Guryeva, O.M. Experimental Study of Self-Preservation Effect of Gas Hydrates in Frozen Sediments. In Proceedings of the 9th International Conference on Permafrost, Fairbanks, AK, USA, 28 June–3 July 2008; Volume 28.
41. Shpolyanskaya, N.A.; Streletskaya, I.D.; Surkov, A. Cryolithogenesis within the Arctic Shelf (Modern and Ancient) (Published in Russian). *Earth's Cryosph.* **2006**, *10*, 49–60.
42. Chuvilin, E.; Bukhanov, B. Effect of Hydrate Formation Conditions on Thermal Conductivity of Gas-Saturated Sediments. *Energy Fuels* **2017**, *31*, 5246–5254. [[CrossRef](#)]
43. Chuvilin, E.M.; Kozlova, E.V.; Skolotneva, T.S. Experimental Simulation of Frozen Hydrate-Containing Sediments Formation. In Proceedings of the Fifth International Conference on Gas Hydrates, Trondheim, Norway, 13–16 June 2005; pp. 1561–1567.
44. Chuvilin, E.M. Migration of ions of chemical elements in freezing and frozen soils. *Polar Record.* **1999**, *35*, 59–66.
45. Chuvilin, E.M.; Ershov, E.D.; Smirnova, O.G. Ionic Migration in Frozen Soils and Ice. In Proceedings of the 7th International Permafrost Conference, Yellowknife, NT, Canada, 23–27 June 1998; pp. 167–171.
46. Lebedenko, Y.P. Cryogenic Migration of Ions and Bound Moisture in Ice-Saturated Frozen Rocks (Published in Russian). *Eng. Geol.* **1989**, *4*, 21–30.
47. Andersland, O.B.; Biggar, K.W. Site Investigations of Fuel Spill Migration into Permafrost. *J. Cold Reg. Eng.* **2002**, *13*, 165–166. [[CrossRef](#)]
48. Ershov, E.D.; She, Z.S.; Lebedenko, Y.; Chuvilin, E.M.; Kryuchkov, K.Y. Mass Transfer and Deformation Processes in Frozen Rocks Interacting with Aqueous Salt Solutions (Published in Russian). In Proceedings of the III Scientific and Technical Workshop “Engineering-Geological Study and Evaluation of Frozen, Freezing and Thawing Soils (IGK-92)”, St. Petersburg, Russia, 1993; pp. 67–77. Available online: <https://istina.msu.ru/publications/article/2627661/> (accessed on 23 April 2019).

49. Winiger, P.; Barrett, T.E.; Sheesley, R.J.; Huang, L.; Sharma, S.; Barrie, L.A.; Yttri, K.E.; Evangeliou, N.; Eckhardt, S.; Stohl, A.; et al. Source Apportionment of Circum-Arctic Atmospheric Black Carbon from Isotopes and Modeling. *Sci. Adv.* **2019**, *5*, eaau8052:1–eaau8052:10. [[CrossRef](#)]
50. Chuvilin, E.M.; Grebenkin, S.I.; Sacleux, M. Influence of Moisture Content on Permeability of Frozen and Unfrozen Soils. *Kriosf. Zemli* **2016**, *20*, 66–72.



© 2019 by the authors. Licensee MDPI, Basel, Switzerland. This article is an open access article distributed under the terms and conditions of the Creative Commons Attribution (CC BY) license (<http://creativecommons.org/licenses/by/4.0/>).